JOURNAL OF GEOPHYSICAL RESEARCH, VOL. 102, NO. D24, PAGES 29,641–29,649, DECEMBER 26, 1997

Formulation of surface heat flux: Application to BOREAS

L. Mahrt,[1] Jielun Sun,[2] J. I. MacPherson,[3] N. O. Jensen,[4] and R. L. Desjardins[5]

Abstract. The aerodynamic temperature is required for prediction of the surface heat flux using Monin-Obukhov similarity. This "fictitious" temperature is not systematically equal to the actual air temperature near the surface and is not directly available from observations or in numerical models. The aerodynamic temperature is normally replaced with either the canopy air temperature or the surface radiation temperature, sometimes accompanied by adjustment of the thermal roughness length or specification of an excess resistance. In this study, the relationship between the aerodynamic temperature and the surface radiation temperature is examined in terms of the surface energy budget and simple representation of canopy structure. Previous inconsistencies are discussed. The observed behavior of the aerodynamic temperature is studied using Canadian Twin Otter aircraft data from BOREAS over nine different forested and nonforested sites. Variation of the behavior of the aerodynamic temperature between different parts of the boreal forest is found to be strongly correlated with the red reflectance.

1. Introduction

Formulation of the surface heat flux is not well posed over most real surfaces because of ambiguity in the definition of the surface temperature. For prediction of moisture fluxes the surface temperature can be eliminated by combining the surface energy budget with the bulk aerodynamic formula, as in the Penman or Penman-Monteith method [*Monteith and Unsworth*, 1990].

Prediction of the surface heat flux is normally posed in terms of a single surface temperature or two separate temperatures representing the canopy and subconopy surfaces. However, definition of the surface temperature(s) from observations is not straightforward. Even with hypothetically perfect information on the temperature distribution for every single leaf, it is not obvious how to define unique canopy temperatures for calculation of heat fluxes. For this reason, the estimation of bulk transfer coefficients or resistances for heat from observations is never unique.

Prediction of the heat flux in terms of multiple surface temperatures can remove some of the inadequacies incurred with use of single surface temperature, as will be noted below. Although the motivation to use multiple surface temperatures seems irresistible, many modeling applications will continue to relate the surface heat flux to a single surface temperature to accommodate required economy and simplicity. Additionally, observational setups often measure only a single surface temperature because of other priorities.

[1]College of Oceanic and Atmospheric Sciences, Oregon State University, Corvallis.
[2]Program in Atmospheric and Oceanic Sciences, University of Colorado, Boulder.
[3]Flight Research Laboratory, National Research Council, Ottawa, Ontario, Canada.
[4]Department of Meteorology and Wind Energy, Risø National Laboratory, Denmark.
[5]Centre for Land and Biological Resource Research, Agriculture Canada, Ottawa, Ontario, Canada.

Paper number 97JD01116.
0148-0227/97/97JD-01116$09.00

The heat flux is related to a single surface "aerodynamic" temperature T_0 using the bulk aerodynamic relationship

$$\overline{w'T'} = C_H V [T_0 - T_{air}] \quad (1)$$

where T_{air} is the time- or space-averaged air temperature in the surface layer (Figure 1), and C_H is the transfer coefficient. To avoid problems with definition of the velocity scale V at weak wind speeds [*Beljaars*, 1995; *Mahrt and Sun*, 1995], the heat flux can also be expressed in terms of an atmospheric conductance g_a or atmospheric resistance r_a in which case

$$\overline{w'T'} = g_a[T_0 - T_{air}] = \frac{1}{r_a}[T_0 - T_{air}] \quad (2)$$

The transfer coefficient, conductance, and resistances are estimated in terms of the Monin-Obukhov similarity theory or derivatives of such theory using the Richardson number [*Mahrt and Ek*, 1984; *Choudhury et al.*, 1986].

Application of such similarity theory requires the surface

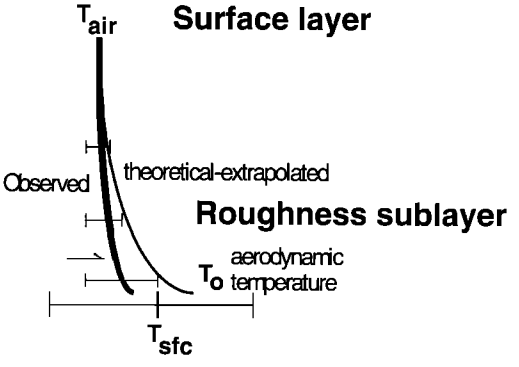

Figure 1. Plausible profiles of extrapolated temperature using Monin-Obukhov similarity theory (thin line on right) and observed temperature profile (thick line on left) and range of the horizontal variation of the averaged observed air and surface temperature (error bars). Actual conditions vary dramatically from case to case, and the averaged surface radiation temperature T_{sfc} may be substantially larger than the aerodynamic temperature T_0.

aerodynamic temperature. This temperature is a fictitious temperature in that it may be quite different from the true air temperature at a fixed level near the surface (Figure 1) depending on the precise definition of the aerodynamic temperature which in turn depends on the method of computing the transfer coefficients (section 2). Normally, the transfer coefficients are estimated in terms of Monin-Obukhov similarity theory which does not accurately describe the temperature profiles in the roughness sublayer immediately above the canopy [*Brutsaert*, 1982]. Theoretically, this is not a difficulty for predicting the heat flux, provided that one can accept an aerodynamic temperature that has only an indirect relationship to the true air temperature near the surface. The heat flux cannot be predicted in terms of the actual air temperature at a fixed height near the surface because there is no one similarity theory that describes temperature profiles both close to the canopy and in the overlying atmospheric surface layer.

The aerodynamic temperature is not available in models and is replaced by the observed surface radiation temperature computed from the surface energy budget. In many observational programs without detailed vertical profiles, the aerodynamic temperature is also unavailable and replaced by the surface radiation temperature. Use of the surface radiation temperature requires adjustment of the transfer coefficient in order to predict the correct heat flux. This adjustment is sometimes implemented by changing the roughness length for heat as an input parameter for application of similarity theory. This adjusted roughness length is referred to as the "radiometric" roughness length, or, equivalently, the roughness length for heat is specified to be equal to that for momentum, and an excess resistance is defined [*Stewart et al.*, 1994; *Stewart*, 1995; *McNaughton and Van Den Hurk*, 1995].

The "radiometric" roughness length for heat is generally specified to be some fraction or function of the roughness length for momentum. This approach does not appear to be promising for most vegetated surfaces where the roughness length for heat is found to depend on many factors [*Kustas et al.*, 1990; *Sun and Mahrt*, 1995a; see additional references by *Mahrt*, 1996] and is sensitive to the way in which the surface radiation temperature is measured. *Sun and Mahrt* [1995a] find that when combining data from different field programs, the radiometric roughness length becomes unrelated to the momentum roughness length.

The transfer coefficient is negative (countergradient flux), and the radiometric roughness length is greater than the observational height when the heat flux is upward, yet the averaged surface radiation temperature is less than the air temperature, as occurred in the work of *Kustas et al.* [1990]. For example, over short agricultural crops, upward heat flux is generated by hot bare soil between the rows, while cooler transpiring crops may cause the averaged surface radiation temperature to be less than the air temperature [*Sun and Mahrt*, 1995a]. Over semiopen forest canopies, upward heat flux is generated by the canopy top that is only slightly warmer than the air temperature, while shaded ground surfaces can cause the averaged surface radiation temperature to be cooler than the air temperature [*Sun and Mahrt*, 1995b].

This problem is reduced by relating the heat flux separately to the canopy and subcanopy temperatures [*Lhomme et al.*, 1994; *Norman et al.*, 1995; *Sun and Mahrt*, 1995b; *Kustas and Humes*, 1996]. Such models follow the earlier resistance geometry of models for the evapotranspiration [*Shuttleworth and Wallace*, 1985; *Dolman*, 1993; see also *Wallace*, 1995, and references therein]. This approach eliminates the countergradient heat flux problem. A set of surface resistances defines the "canopy source height" air temperature (Figure 2a) which is assumed to be the true air temperature in the canopy. These resistances define the heat flux between the canopy leaf surface and the canopy air and between the ground or understory and the canopy air (Figure 2a). The heat flux above the canopy is then computed from (2) by determining the resistance above the canopy from Monin-Obukhov similarity theory. Unfortunately, this computation requires that the canopy source air temperature be equal to the aerodynamic temperature in order that similarity theory be applied. Since the aerodynamic temperature is a fictitious temperature resulting from extrapolation of the similarity profile down to the roughness height, the two uses of the canopy air temperature are in conflict. Therefore existing models are inconsistent.

The present study defines the aerodynamic temperature as that surface temperature which predicts the correct heat flux in (1) or (2), given the atmospheric transfer coefficient determined from Monin-Obukhov similarity theory (section 2). The roughness length for heat is eliminated as an adjustable parameter by specifying it to be equal to the roughness length for momentum; this precisely defines the aerodynamic temperature used in this study (section 2). Equivalently, we could have related the heat flux to the surface radiation temperature and introduced an adjustable excess resistance which, for the present data, must be allowed to take on negative values. The excess resistance and aerodynamic relationship are mathematically related and one can be computed from the other (section 2.1).

We summarize by noting that the surface heat flux can be

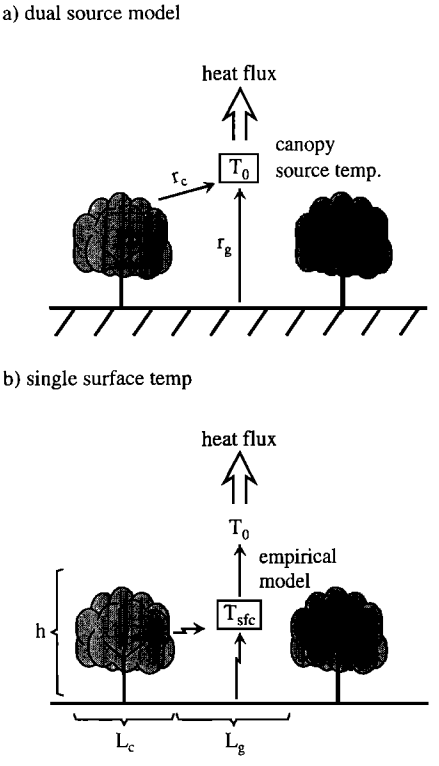

Figure 2. (a) Equating the aerodynamic temperature to the canopy source temperature in the two-source canopy model and (b) empirically relating the aerodynamic temperature to the average surface radiation temperature (section 2.2).

formulated using Monin-Obukhov similarity theory and a single surface temperature by (1) predicting the thermal roughness length, (2) specifying an excess resistance, and (3) modeling the aerodynamic temperature.

The first two approaches suffer problems particularly with partial vegetation cover, while the third approach is unproven. In this study, we examine the behavior of the aerodynamic temperature from observations toward the eventual goal of modeling the aerodynamic temperature.

The relationship between the aerodynamic temperature and the surface radiation temperature will be examined in terms of heat fluxes spatially averaged from Canadian Twin Otter aircraft measurements during the Boreal Ecosystem-Atmosphere Study (BOREAS). Most flight tracks extend over a region of a single dominant tree species but also include smaller populations of secondary species and may include some variations of tree age and height. Additional tracks encompass burned and cleared areas and an agricultural region. The formulation of spatially averaged fluxes are more applicable to numerical models than point measurements; however, information on the canopy is limited to aircraft remotely sensed data.

The next section derives a theoretical expression for the aerodynamic temperature. Using data described in section 3, the relationship between the aerodynamic temperature and the surface radiation temperature is studied in sections 4 and 5.

2. Aerodynamic Temperature

2.1. Relation to Surface Radiation Temperature

The aerodynamic temperature can be estimated from observations in the following ways: (1) using similarity theory, extrapolate the temperature profile downward from the surface layer to the roughness length for momentum [*Huband and Monteith*, 1986; *Beljaars and Holtslag*, 1991]; (2) given the atmospheric resistance from similarity theory, determine the aerodynamic temperature T_0 from the observed heat flux and air temperature using the relationship

$$\overline{w'T'} = \frac{[T_0 - T_{air}]}{r_a} \tag{3}$$

This general approach was applied by *Choudhury et al.* [1986] using the heat flux computed as a residual from the surface energy balance and by *Kustas* [1990] using eddy correlation measurements of the heat flux.

Equation (3), as written, still does not clearly define the aerodynamic temperature since the atmospheric resistance in the literature is computed in several different ways. We have estimated r_a in three different ways: (1) r_{ah} based on the stability functions for heat from *Paulson* [1970], (2) r_{am} based on the stability functions for momentum from *Paulson* [1970], and (3) r_{am} estimated from the observed surface friction velocity u_* when available, as in the works of *Lee and Black* [1993], *Jensen and Hummelshøj* [1995], and others, as

$$r_{am} = \frac{u}{u_*^2} \tag{4}$$

For the third approach, specification of the roughness height and stability function are not required. Using the data described in section 3, we found that the differences between the three calculations of the aerodynamic temperature are usually less than 0.2°C with an extreme value reaching 0.3°C. These differences are small compared to the errors in the rest of the analysis (section 3). We adopt the simpler approach and define the aerodynamic temperature in terms of (4). Then, the aerodynamic temperature becomes the single tunable parameter for the heat flux, and the stability function and roughness length for heat are eliminated from the calculation. Equations (3) and (4) mathematically define the aerodynamic temperature for this study.

Recall that application of Monin-Obukhov similarity theory requires that the surface air temperature be defined as the aerodynamic temperature which may be quite different from any observable temperature at a fixed level near the surface and may be quite different from the surface radiation temperature. However, models either replace the aerodynamic temperature with the surface radiation temperature or a canopy air temperature. In this section, we will make the usual assumption that the aerodynamic temperature and canopy air temperature are the same. The actual behavior of the aerodynamic temperature will be examined from observations in sections 4 and 5.

The surface heat flux is sometimes related to the surface radiation temperature and some temperature outside the molecular sublayer by defining a surface resistance such that

$$\overline{w'T'} = \frac{1}{r_s}[T_{sfc} - T_0] = g_s[T_{sfc} - T_0] \tag{5}$$

where g_s and r_s are the surface conductance and surface resistance, respectively, where again T_0 is assumed to be both the aerodynamic temperature and the canopy air temperature. In canopy models, (5) is sometimes applied separately to the canopy top and the ground surface using the respective surface radiation temperatures (Figure 2a). This procedure uses a common single canopy air temperature for both components of the heat flux.

The aerodynamic temperature can be eliminated by matching the heat flux values from (2) and (5), in which case

$$\overline{w'T'} = \frac{1}{r_a + r_s}[T_{sfc} - T_{air}] \tag{6}$$

Normally the atmospheric resistance r_a would be determined from similarity theory in which case (6) becomes a defining relationship for the resistance r_s. This resistance is sometimes referred to as the excess resistance (Introduction). If one equates r_a with r_{ah}, then specifying the excess resistance replaces adjustment of the thermal roughness height which is equated to the momentum roughness height. *Stewart et al.* [1994] attributes r_s to corrections required because of (1) use of the surface radiation temperature instead of the aerodynamic temperature and (2) use of the atmospheric resistance for momentum instead of the atmospheric resistance for heat.

Norman and Becker [1995] define the excess resistance by using the aerodynamic temperature and r_{ah} in (6) in which case the only role of the excess resistance is to account for the difference between the roughness lengths for heat and momentum. In this case, the aerodynamic temperature and excess resistance are both unknowns, and an additional assumption or relationship is needed to close the system. Still other definitions of the excess resistance and aerodynamic temperature can be found in the literature. *McNaughton and Van Den Hurk* [1995] survey attempts to estimate the excess resistance from existing data sets, emphasizing observation inadequacies.

Matching (3) with (6) defines the relationship between the

aerodynamic temperature, surface radiation temperature, and excess resistance. That is, adjusting the aerodynamic temperature or applying an excess resistance are equivalent. If the averaged surface radiation temperature is greater than the aerodynamic temperature with upward heat flux, then the excess resistance is positive. If the averaged surface radiation temperature is smaller than the aerodynamic temperature with upward heat flux, then the excess resistance is negative.

Alternatively, (2) can be expanded as

$$\overline{w'T'} = \frac{1}{r_a}[(T_0 - T_{sfc}) + (T_{sfc} - T_{air})] \tag{7}$$

The temperature difference $T_{sfc} - T_{air}$ is normally available from observations and is always available from numerical models, while the temperature difference $T_0 - T_{sfc}$ must be parameterized.

The temperature difference $T_0 - T_{sfc}$ is constrained by the surface energy balance. Using (6), the surface energy balance at the leaf or ground surface with surface temperature T_{sfc} can be written as

$$\rho c_p \frac{1}{r_s}[T_{sfc} - T_0] = E_{net} - F_s \tag{8}$$

where

$$E_{net} \equiv S(1 - \alpha) - Q_L + \varepsilon L - \varepsilon\sigma T_{sfc}^4 \tag{9}$$

and F_s is the heat flux into the ground. The left-hand side of (8) is the sensible heat flux $\rho c_p \overline{w'T'}$, Q_L is the latent heat flux, L is the downward longwave radiation, ε is the emissivity, F_s is the flux of heat into the surface, and again, r_s is the surface resistance. In section 4, (8) is used as a starting point for analysis of aircraft observations.

2.2. Surface Resistance

Often, the surface resistance is related to the growth of the molecular sublayer over individual leaves. Within the concept of the total heat flux, this approach makes the "big leaf" assumption. This approach also assumes that the air temperature is sufficiently mixed in the canopy and that the air temperature at the outer edge of the molecular sublayer can be represented by a single canopy air temperature. This canopy air temperature is then again equated to the aerodynamic temperature T_0 in order to use similarity theory above the canopy. Then the heat flux in the molecular sublayer adjacent to the leaf surface can be expressed in terms of the thermal conductivity κ_T and the bulk temperature gradient such that

$$\overline{w'T'} = \alpha \frac{\kappa_T}{\delta}[T_{sfc} - T_0] \tag{10}$$

in which case the surface resistance in (8) becomes

$$r_s = \frac{\delta}{\alpha\kappa_T} \tag{11}$$

where δ is the depth of the molecular sublayer and α is a nondimensional coefficient.

To estimate the depth of the molecular sublayer, we follow the approach of *Jensen and Hummelshøj* [1995]. For flow over individual leaf surfaces or other roughness elements, a molecular boundary layer forms over the element and grows as $(\nu t)^{1/2}$ when following the flow in the downstream direction. This thickness scales with the viscosity instead of the conductivity since it estimates the depth where turbulent transport is unimportant. Here, one assumes that the depth of the molecular sublayer is determined by the element size rather than the timescale of the transporting eddies as in the surface renewal theory. The timescale for the flow to transverse the element of width b scales as b/u_* where the wind speed scale in the roughness layer is assumed to be proportional to u_*. Then, the depth of the molecular sublayer δ can be expressed as $(C\nu b/u_*)^{1/2}$ where C is an undetermined coefficient. Substituting this estimate of the molecular sublayer depth into the expression for surface resistance (equation (11)),

$$r_s = \left(\frac{C\nu b}{u_*\kappa_T^2}\right)^{1/2} \tag{12}$$

This formulation is untested. However, the unknown value of C can be estimated by introducing a drag coefficient C_D, in which case (12) becomes

$$r_s = \left(\frac{b}{C_* u}\right)^{1/2} \tag{13}$$

where u is the wind speed at a standard level in the surface layer and

$$C_* \equiv \frac{(C_D)^{1/2}\kappa_T^2}{C\nu} \tag{14}$$

Equation (13) has been used by *Jones* [1983], *Raupach and Finnigan* [1988], and *Choudhury and Monteith* [1988]. On the basis of idealized surfaces in laboratory flow, C_* is estimated to be 6.62 $m^2\ s^{-1}$. For real leaf surfaces in a turbulent atmosphere this value may be somewhat larger corresponding to smaller surface resistance [*Jones*, 1983]. Furthermore, these relationships must be applied as bulk parameterizations collectively representing all of the leaves of various orientations and positions within the canopy.

Solving for the temperature difference from (10) and using (12) to estimate the molecular sublayer depth, we obtain

$$T_{sfc} - T_0 = \frac{\overline{w'T'}(C\nu b)^{1/2}}{\alpha\kappa_T(u_*)^{1/2}} \tag{15}$$

The temperature difference is proportional to the heat flux and inversely proportional to the square root of the friction velocity. Larger u_* corresponds to more mixing in the canopy and reduced air-leaf temperature difference. Similarly, *Beljaars and Holtslag* [1991] estimate the aerodynamic temperature by extrapolating the observed temperature profile to the roughness height for momentum and find that the temperature difference $[T_{sfc} - T_0]$ is proportional to the heat flux scaled by the surface friction velocity. Equation (15) also predicts that larger element size b leads to thicker molecular sublayers and therefore greater temperature difference. Equation (15) will be used as guidance for interpreting the behavior of the observed temperature difference in section 4.

Equation (15) becomes more difficult to interpret for partial canopy cover or bare ground surface. In the latter case, b is essentially infinity. With large b the element size is no longer relevant and the timescale of the renewal due to scouring of the molecular sublayer by eddies becomes the governing factor.

3. BOREAS Data

3.1. Fluxes

This study analyzes data collected by the Twin Otter research aircraft from the Canadian National Research Council [*MacPherson*, 1996]. The data were collected with repeated runs over fixed tracks representing different "homogeneous" subareas during BOREAS [*Sellers et al.*, 1995]. The air temperature T_{air}, observed at the aircraft level (~35 m), has been converted to a local potential temperature by adding 0.01 (°C/m)z where z is the height of the aircraft level. Air temperature and surface radiation temperature are averaged along the flight track for each pass. Flux values for individual passes are significantly contaminated by random flux sampling errors. Some of the track lengths are quite short (Table 1, section 4). Therefore fluxes are averaged over all of the passes over the same track for a given flight day. This defines a "case" or data point in the discussions below. Generally, all of the repeated passes for a given day and given site occur within a 1 hour period in which case the heat flux and air temperature vary by only a small amount. However, the surface radiation temperature can change significantly during a 1 hour period since small changes of the Sun angle can significantly change the fraction of shaded ground surface, as discussed below.

Derived quantities, such as roughness length, Obukhov length, and aerodynamic temperature are computed from such averaged fluxes. The roughness length for momentum for each site (section 3) is computed from observed fluxes and the similarity relationship of *Paulson* [1970]. Near-neutral cases are emphasized in the determination of the roughness length in order to minimize the influence of the particular form of the stability function of the similarity theory. The aerodynamic temperature is computed for each flight over a given site using (3)–(4). All of the flight-averaged values for the different sites are combined into one collection of 38 cases.

In addition, 15 runs over an agricultural area south of the boreal forest will be analyzed for some specific comparisons in section 4. Most of these runs occurred on separate days. Although the flight track was approximately 20 km, the random flux error was still significant because of only a single pass over the track. Some of the analysis below uses the agricultural data averaged over three periods, the late spring period when much of the area is bare soil and emerging crops, midsummer period when much of the area is covered with green crops dominated by canola and summer wheat, and the late summer period when much of the crop was senescent or harvested.

3.2. Surface Radiation Temperature

Since the field of view of the Barnes PRT-5 is about 5 m across, it can simultaneously include shaded and sunny ground surfaces with temperature contrasts of more than 10°C. Interpretation of the radiometer data must account for instrumental averaging of the upward longwave radiation over the heterogeneous field of view of the instrument window. We will neglect the fact that use of nadir (zero zenith angle) measured upward longwave radiation can lead to significant errors as an estimate of the hemispheric emission and, consequently, significant errors in the surface energy budget [*Otterman et al.*, 1995, and others]. We will also neglect any inadvertent weighting within the window which depends on the details of the radiometer. Even without such complications, the temperature from the measured radiation does not correspond to the linearly averaged temperature over the field of view of the radiometer. For example, consider a surface with J surface types that occupy the field of view of the ith observation from the radiometer. Then the ith observation of the radiometer can be written as

$$\varepsilon T_{\mathrm{sfc},i}^4 = \sum_{j=1}^{J} f_{ij}\varepsilon_j T_{ij}^4 \tag{16}$$

where f_{ij} is the fractional coverage of the jth surface type for the ith observation as seen by the radiometer, ε_j the longwave emissivity for the jth surface type, and T_{ij} the temperature for the jth surface type for the ith observation; ε is the emissivity of the field of view. For example, the different surface types seen by the radiometer might be sunny canopy top, shaded ground surface, and sunny ground surface.

The temperature of each surface type T_{ij} is decomposed into the surface temperature linearly averaged over the field of view $\bar{T}_i$ and the perturbation from this temperature, T'_{ij}, where

$$\overline{T_i} = \sum_{j=1}^{J} f_{ij}T_{ij} \tag{17}$$

The magnitude of T'_{ij} is proportional to the degree of surface heterogeneity which could in turn be proportional to the size of field of view of the instrument. Assuming that the surface emissivity is near unity with small spatial variations, the measured longwave radiation can be written to leading order as

$$\varepsilon T_{\mathrm{sfc},i}^4 \approx \sum_{j=1}^{J} f_{ij}\varepsilon_j(\bar{T}_i^4 + 3\bar{T}_i^3 T'_{ij} + 6\bar{T}_i^2 T'^2_{ij}) \tag{18}$$

For most of the BOREAS data the radiometer sees very little bare soil, and the emissivity of the ground cover and the tree canopy are thought to be about 0.98. The influence of variable emissivity appears to be small [*Norman and Becker*, 1995]. For constant emissivity the first-order perturbation term T'_{ij} sums exactly to zero in which case

$$T_{\mathrm{sfc},i}^4 \approx \bar{T}_i^4 \sum_{j=1}^{J} f_{ij}\left(1 + \frac{6T'^2_{ij}}{\bar{T}_i^2}\right) \tag{19}$$

where we have assumed that the emissivity used on the left-hand side of (18) is the same as the spatially averaged emissivity. Choosing an extreme example where the field of view is half shaded ground and half sunny ground ($f_{i1} = f_{i2} = 0.5$) and choosing the shaded ground temperature to be 15°C and the sunny ground temperature to be 35°C [*Sun and Mahrt*, 1995b], the error in the estimated linearly averaged temperature is about 0.6°C. The expected resolution of the radiometer calibration is about 1°C.

3.3. Visible and Near-infrared Radiation

Section 4 will make use of the reflected red radiation and the normalized difference vegetation index (NDVI) computed from the Skye Industries vegetation greenness indicator mounted on the Twin Otter aircraft. The red band is centered on 660 μm and the near-infrared band is centered on 730 μm. The red reflectance is found to be a useful measure of surface state (section 5). Unfortunately, the measurement of downward red radiation malfunctioned on several flights and seemed to suffer from errors associated with correction for aircraft attitude angles. Here we normalize the reflected red

Table 1. Flight Path Length L (km), Site-Averaged Air-Surface Temperature Difference, Roughness Height for Momentum (Section 3), Site-Averaged Difference Between Surface Temperature and Aerodynamic Temperature $T_{sfc} - T_0$, NDVI, and Pseudo Red Reflectance (Section 3) (10^{-3})

Site	L	$T_{sfc} - T_{air}$	z_{om}, m	$T_{sfc} - T_0$	NDVI	RR
Young jack pine, n	2.5	4.5	1.5	2.2	0.41	4.8
Burn north	11	4.2	0.8	2.1	0.42	5.5
Old jack pine, n	3	2.3	1.0	0.5	0.41	4.4
Old jack pine, s	6	1.3	1.8	−0.5	0.38	4.0
Old black spruce, n	10.5	0.5	1.4	−1.4	0.43	3.6
Old black spruce, s	14.5	−0.1	1.3	−1.8	0.39	3.8
Old aspen	11	0.0	3.0	−1.7	0.52	4.3
Av May	20	2.3	0.06	0.4	0.31	8.6
Av July	20	0.7	0.20	−1.3	0.43	5.6
Av September	20	4.1	0.05	1.6	0.09	17.0

The "n" refers to the northern study area and "s" refers to the southern study area. The averaged downward solar radiation ranged from 609 Wm^{-2} at old jack pine north to 708 Wm^{-2} at old jack pine south. When eliminating flights with partial cloud cover, the values of $T_{sfc} - T_{air}$ and $T_{sfc} - T_0$ both increase by about 1° for most sites. Ag, agricultural.

radiation by the better behaved incoming radiation S and form a pseudo red reflectance

$$RR \equiv \frac{\text{reflected red}}{S} \tag{20}$$

4. Relationship of Aerodynamic Temperature to Surface Radiation Temperature

Huband and Montieth [1986] and *Kustas* [1990] have estimated the aerodynamic temperature from observations and studied the relationship between the aerodynamic temperature and the observed surface radiation temperature. Over winter wheat, *Huband and Monteith* [1986] found that the surface radiation temperature became cooler than the aerodynamic temperature on a windy day when deformed wheat plants exposed cool bare soil to the radiometer measurement. Over a partial canopy cover, *Kustas* [1990] found that the surface radiation temperature became significantly larger than the aerodynamic temperature with high solar elevation angle and associated large fraction of sunlit bare soil.

4.1. Averages for Different Sites

The errors in the surface-air temperature differences are thought to be of the order of 1°C, so differences between sites less than 1°C may not be significant. The variation of the air-surface temperature difference between different sites in Table 1 can be interpreted in terms of the canopy geometry. For semiopen canopies with taller trees, such as old aspen and old black spruce, the averaged surface temperature is strongly influenced by shaded ground and is therefore not significantly larger than the air temperature and is often smaller than the aerodynamic temperature. However, for more sparse canopies with shorter trees, much of the ground or understory surface is sunny at midday, as occurs for the burn and the young jack pine sites. For these sites, the warm temperatures of the open sunny ground lead to larger values of $T_{sfc} - T_{air}$ and $T_{sfc} - T_0$.

The "loose" relationship between the heat flux and the surface radiation temperature is evident in Figure 3, which shows the run-to-run variation of air, surface, and aerodynamic temperatures for different flights over the black spruce sites. In general, the surface radiation temperature is more variable than the aerodynamic temperature. The time variation of the surface radiation temperature shows a variety of signatures not directly related to the heat flux (Figure 3) due to the influence of changing Sun angle on the fraction of shaded ground surface. For example, July 21 in the top panel corresponds to early afternoon conditions where the heat flux and air temperature vary slowly, but the averaged surface radiation temperature decreases rapidly with time due to the influence of increasing fraction of shaded ground surface. With lower Sun angle, the surface radiation temperature is much cooler than the aerodynamic temperature even though the heat flux is upward. Similar situations occur on July 25 and September 15 when flights were carried out in the afternoon.

The heat flux is always upward, so the aerodynamic temper-

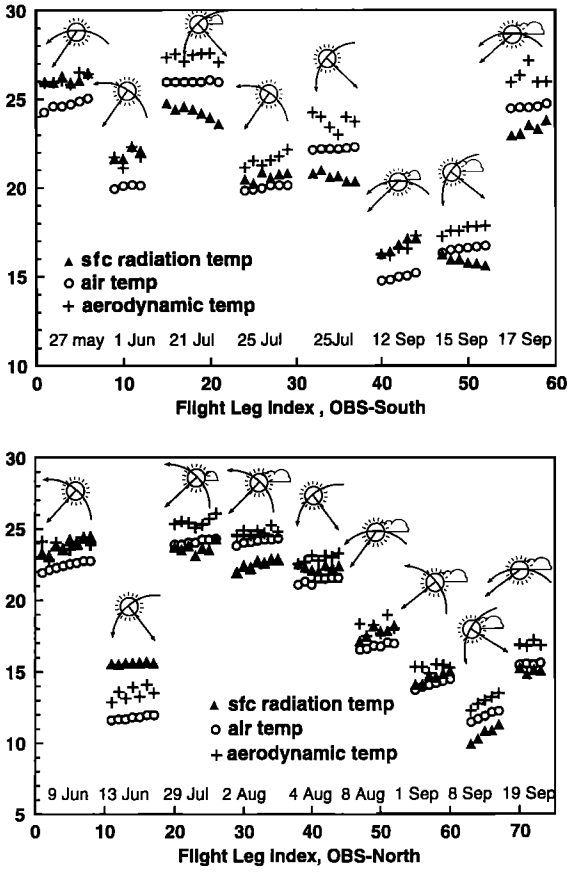

Figure 3. Pass-averaged surface radiation temperature (triangles), air temperature (circles), and the aerodynamic temperature (pluses) computed from run-averaged fluxes for different flights over the old black spruce site in the southern (OBS-S) and northern study areas (OBS-N). The horizontal axis is an arbitrary run number. The arrows directed from the Sun toward the surface indicates the solar zenith angle. The curved arrows directed counterclockwise indicate whether the Sun elevation angle is increasing with time in the morning, contains a noon time maximum during the flight period (curved arrow is symmetric) or decreasing with time in the afternoon. A small cloud indicates reduction of incoming solar radiation of more than 100 Wm^{-2}, while a large cloud indicates a reduction of more than 300 Wm^{-2} (see section 3).

ature is always warmer than the air temperature. Consider the following scenarios:

$T_{sfc} < T_{air}$. For 7 of the 17 cases the averaged surface radiation temperature is smaller than the air temperature corresponding to countergradient flux based on surface radiation temperature (negative excess resistance or undefined radiometric roughness height).

$T_{sfc} \approx T_{air} < T_0$. For several cases the averaged surface radiation temperature is about the same as the air temperature but smaller than the aerodynamic temperature corresponding to very small total resistance, negative excess resistance, and very large radiometric roughness height.

$T_{air} < T_{sfc} < T_0$. For some cases the averaged surface radiation temperature is greater than the air temperature but less than the aerodynamic temperature corresponding to negative excess resistance and radiometric roughness height greater than the momentum roughness length.

$T_{sfc} > T_0$. For June 13, the averaged surface radiation temperature is greater than the aerodynamic temperature corresponding to positive excess resistance, and the radiometric roughness length is smaller than the momentum roughness length.

Statistically considering all of the sites, the averaged surface radiation temperature is more likely to be cooler than aerodynamic temperature with partly cloudy conditions as opposed to clear skies. Partial cloud shading of the surface lowers the averaged surface radiation temperature, while the spatially averaged heat flux remains upward due to the flux from sunny areas. The cases in Figure 3 where the averaged surface radiation temperature is less than the air temperature occur either with low Sun angle or with partial cloud cover. Note that the Sun angle effect is related to microscale variations, while the cloud effect is more related to small mesoscale variations within the averaging area. Cloud effects are not explicitly included in this study.

4.2. Relationship to the Surface Energy

For the present data, the temperature difference $T_{sfc} - T_0$ is closely related to the incoming solar radiation. The incoming solar radiation determines the temperature of the sunlit part of the canopy which accounts for most of the heat flux. In contrast, the understory may play a relatively more significant role for the moisture flux [*Lee and Black*, 1993].

Section 2 motivates relating the aerodynamic-surface temperature difference to the net radiation minus the latent heat flux (E_{net}, equation (9)). The overall dependence of the temperature difference on E_{net} is evident by averaging the value of $T_{sfc} - T_0$ for different intervals of E_{net} for each site (Figure 4). For a given site, the temperature difference generally increases with increasing E_{net}.

The variation of $T_{sfc} - T_0$ between sites is substantial (Figure 4). Values of $T_{sfc} - T_0$ from the agricultural, burn, and young jack pine areas are large compared with those of the more forested old jack pine, old black spruce, and old aspen sites. The first group of sites consists of low crops or short trees with significant open sunny ground surface. These locations are characterized by less shade compared to the older forested sites. As a result, the downward pointing radiometer views less shade, and T_{sfc} is higher for a given heat flux (given T_0), and $T_{sfc} - T_0$ is larger for a given value of E_{net}.

This shading effect is zero with completely bare soil, increases with partial vegetation, and probably becomes small with a dense upper canopy where little shaded ground surface

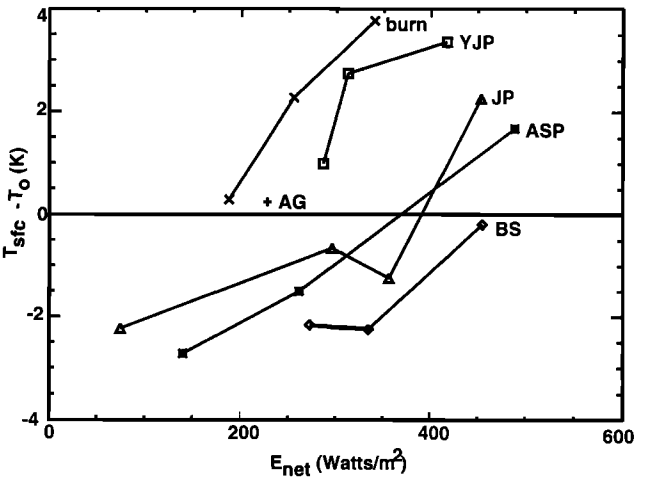

Figure 4. Site-averaged values of the temperature difference $T_{sfc} - T_0$ for different values of the net energy E_{net} for the burn, young jack pine (YJP), old jack pine (JP), aspen (ASP), and black spruce (BS) tracks.

is seen from nadir. The NDVI captures the large variation of surface radiation temperature between hot sunny bare ground and cool sunny transpiring green vegetation [*Sun and Mahrt*, 1994]. As a result, the NDVI accounts for almost all of the seasonal variation of $T_{sfc} - T_0$ for the agricultural area. The NDVI also captures some of the seasonal variation of $T_{sfc} - T_0$ for the old aspen site (not shown). *Brunet et al.* [1991] shows that use of the surface radiation temperature overestimates the heat flux significantly when the leaf area index is small, which can be interpreted as large positive values of $T_{sfc} - T_0$ when the NDVI is small.

However, *Goward et al.* [1994] finds that the NDVI is a rather incomplete representation of the vegetation when simultaneously considering a variety of communities ranging from wet coastal forests to semiarid juniper. For the boreal forest the NDVI does not vary significantly between the different sites even though the surface heat and moisture fluxes vary substantially between the different sites. Therefore the NDVI is not a good predictor of the heat flux and aerodynamic temperature.

5. Relationship Between Aerodynamic Temperature and Reflected Red Radiation

For the present data, the reflected red radiation (Figure 5) is a much better predictor of $T_{sfc} - T_0$ than the NDVI. Chlorophyll is a strong absorber of red radiation [*Tucker*, 1979; *Yoder and Waring*, 1994]. Therefore large reflected red radiation implies sunlit nontranspiring surfaces that are generally warmer than transpiring surfaces and act to increase the averaged surface radiation temperature. As an additional factor, shaded ground surface viewed from nadir can substantially reduce the total red reflectance [*Graetz and Gentle*, 1982]. For black spruce forests, *Hall et al.* [1995] find that the largest nadir values of red reflectance correspond to open sunny areas covered mostly with sphagnum moss (limited chlorophyll), while smaller red reflectance occurs for the sunny forest canopy top and shaded ground surfaces. In their study, the red reflectance for sparse black spruce decreases with increasing tree density (up to a critical density) due to increasing shaded ground. The

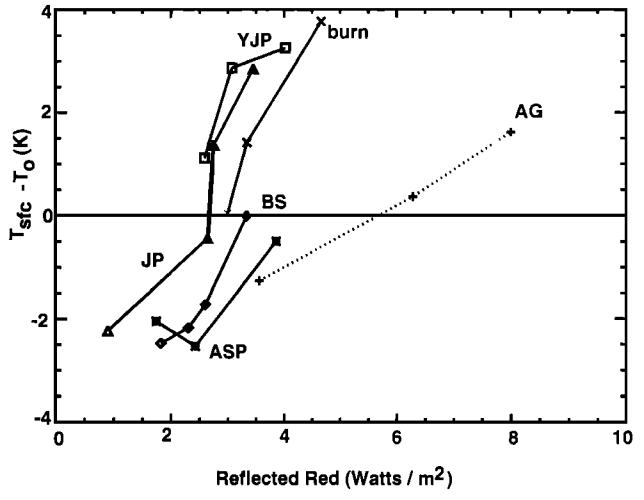

Figure 5. Site-averaged values of the temperature difference $T_{sfc} - T_0$ for different intervals of reflected red radiation (Wm^{-2}). For the agricultural site, the reflected red radiation is largest in the late summer period and is smallest during the midsummer growing season. Track abbreviations are given in Figure 4.

NDVI responds less to changes in shaded fraction since changes in reflected red and near infrared partially cancel. As a result, the NDVI is unable to effectively discriminate between more open forests and more closed forests.

In the black spruce forests the sunlit sphagnum moss reaches very warm temperatures [*Sun and Mahrt*, 1995b] acting to increase the averaged surface radiation temperature. Therefore the averaged surface radiation temperature increases with increasing red reflectance. Because the total heat flux and aerodynamic temperature T_0 are not so sensitive to the shaded ground fraction, the temperature difference $T_{sfc} - T_0$ also increases with red reflectance. The warm sunny moss surface increases the average surface radiation temperature without significantly increasing the total heat flux because of small conductance between the subcanopy ground surface and the air above the canopy.

The strong relationship between the surface radiation temperature and the red reflectance apparently also applies to the jack pine forests (F. Hall, personal communication, 1996) where the lichen-covered ground surface is a strong reflector of red radiation, similar to the moss. The relationship between the temperature difference $T_{sfc} - T_0$ and the red reflectance becomes more obscure for the nonconifer sites.

Nonetheless, the temperature difference $T_{sfc} - T_0$ increases rapidly with reflected red radiation for the nonconfier sites as well as the conifer sites (Figure 5). Although the relationship is excellent for the agricultural data, the $T_{sfc} - T_0$ values are lower than the other sites. This difference is thought to be partly due to the lower Sun angle for the agricultural flight legs which were carried out at the beginning or the end of the flight day. The reflected red radiation (section 3) corresponding to the 660 nm channel (section 3), alone, explains 45% of the variance of $T_{sfc} - T_0$ as compared with 20% explained by E_{net} and only a few percent explained by the NDVI. The 45% value is particularly large considering the uncertainty of the calculation of T_0 and the various errors discussed above. The reflected red radiation combines information on the nature of the surface, fraction of sunlit ground surface, and intensity of incoming solar radiation. The variance explained is higher when using the red channel from the aircraft-mounted satellite simulator data collected in the red channel (597–700 nm) corresponding to the red MSS channel on Landsat. These data were available for 24 cases and explained 67% of the variance of $T_{sfc} - T_0$. For the same data the reflected red radiation measured by the 660 nm channel explained 54% of the variance. Perhaps the wavelengths of the two channels for the vegetation index are too close together. Use of pseudo red reflectance (section 3) removes the influence of variable incoming solar radiation and reduces the variance explained by about one half.

The reflected red radiation might be useful for constructing spatially averaged heat fluxes. However, for application of satellite data the red reflectance is more vulnerable to atmospheric effects than the NDVI. Such atmospheric effects will be much greater for satellite data compared to use of low-flying aircraft in the present study.

6. Conclusions

Most large-scale and operational numerical models relate the surface heat flux to a single surface temperature which is usually the surface radiation temperature computed from the surface energy balance. More sophisticated canopy models relate the heat flux to the canopy air temperature. However, both approaches commit inconsistencies since application of similarity theory requires these temperatures to be equal to the aerodynamic temperature of the air at the roughness height. The use of remotely sensed surface radiation temperature to predict the heat flux is quite complex over the boreal forest because of the influence of shaded subcanopy surfaces which occupy part of the field of view of the radiometers.

On the basis of flux measurements from the Canadian Twin Otter over the boreal forest, the aerodynamic-surface temperature difference is related to the net radiation less the evapotranspiration, as motivated in section 2. However, the scatter is large and the relationship varies substantially between different types of vegetation. The influence of vegetation type on the aerodynamic-surface temperature difference is much better represented by the reflected red radiation than the NDVI. The red reflectance statistically includes the influence of shaded ground surface on the averaged surface radiation temperature and better distinguishes between the canopy and the understory.

This work forms the basis for future development of a model of the aerodynamic temperature. If such a model can be constructed, the present inconsistent application of Monin-Obukhov similarity temperature in numeral models could be avoided.

Acknowledgments. The valuable comments of Yeves Brunet, Bill Kustas, Francois Becker, John Stewart, and Forrest Hall are greatly appreciated. This work is supported by NASA grant NAG 5-2300 and ATM-9310576 from Physical Meteorology Program of the National Science Foundation and by the European Commission's Climate Research Programme, contract EV5V-CT93-0276.

Part of this work was conducted in the Department of Meteorology and Wind Energy, Risø National Laboratory, Denmark, and Centre for Land and Biological Resource Research, Agriculture Canada, Ottawa.

References

Beljaars, A. C., The parametrization of surface fluxes in large scale models under free convection, *Q. J. R. Meteorol. Soc.*, *121*, 255–270, 1995.

Beljaars, A. C. M., and A. A. M. Holtslag, Flux parameterization over land surfaces for atmospheric models, *J. Appl. Meteorol.*, *30*, 327–341, 1991.

Brunet, Y., K. T. Paw U, and L. Prévot, Using the radiative surface temperature in energy budget studies over plant canopies, paper presented at the Fifth International Colloquium on Physical Measurements and Signatures in Remote Sensing, Eur. Space Agency, Courchevel, France, Jan. 1991.

Brutsaert, W. H., *Evaporation Into the Atmosphere*, 299 pp., D. Reidel, Norwell, Mass., 1982.

Choudhury, B. J., and J. L. Monteith, A four-layer model for the heat budget of homogeneous land surfaces, *Q. J. R. Meteorol. Soc.*, *114*, 373–398, 1988.

Choudhury, B. J., R. J. Reginato, and S. B. Idso, An analysis of infrared temperature observations over wheat and calculation of latent heat flux, *Agric. For. Meteorol.*, *37*, 75–88, 1986.

Dolman, A. J., A multiple-source land surface energy balance model for use in general circulation models, *Agric. For. Meteorol.*, *65*, 21–45, 1993.

Goward, S. N., K. R. Huemmrich, and R. H. Waring, Visible-near infrared spectral reflectance of landscape components in western Oregon, *Remote Sens. Environ.*, *47*, 190–203, 1994.

Graetz, R. D., and M. R. Gentle, The relationships between reflectance in the Landsat wavebands and the composition of an Australian semi-arid shrub rangeland, *Photogramm. Eng. Remote Sens.*, *48*, 1721–1730, 1982.

Hall, F. G., Y. E. Shimabukuro, and K. F. Huemmrich, Remote sensing of the forest biophysical structure using moisture decomposition and geometric reflectance models, *Ecol. Appl.*, *5*, 993–1013, 1995.

Huband, N. D. S., and J. L. Monteith, Radiative surface temperature and energy balance of a wheat canopy, *Boundary Layer Meteorol.*, *36*, 1–17, 1986.

Jensen, N. O., and P. Hummelshøj, Derivation of canopy resistance for water vapour fluxes over a spruce forest, using a new technique for the viscous sublayer resistance, *Agric. For. Meteorol.*, *73*, 339–352, 1995.

Jones, H. G., *Plants and Microclimate*, Cambridge University Press, New York, 1983

Kustas, W. P., Estimates of evaporation with a one- and two-layer model of heat transfer over partial canopy cover, *J. Appl. Meteorol.*, *29*, 704–715, 1990.

Kustas, W. P., and K. S. Humes, Sensible heat flux from remotely sensed data at different resolutions, in *Scaling up in Hydrology Using Remote Sensing*, pp. 127–146, edited by J. B. Stewart E. T. Engman, R. A. Feddes, and Y. Kerr, John Wiley, New York, 1996.

Kustas, W. P., B. J. Choudhury, Y. Inoue, P. J. Pinter, M. S. Moran, R. D. Jackson, and R. J. Reginato, Instantaneous and daily values of the surface energy balance over agricultural fields using remote sensing and a reference field in an arid environment, *Remote Sens. Environ. V*, *32*, 125–141, 1990.

Lee, X., and T. A. Black, Atmospheric turbulence within and above a douglas-fir stand, II, Eddy fluxes of sensible heat and water vapour, *Boundary Layer Meteorol.*, *64*, 369–390, 1993.

Lhomme, J.-P., B. Monteny, M. Amadou, A. Chehbouni, and D. Troufleau, Determination of sensible heat flux over Sahelian fallow savannah using infra-red thermometry, *J. Fluid Mech.*, *68*, 93–106, 1994.

MacPherson, J. I., NRC Twin Otter operations in BOREAS 1994, *Rep. LTR-FR-129*, Natl. Res. Council of Can., Ottawa, 1996.

Mahrt, L., The bulk aerodynamic formulation over heterogeneous surfaces, *Boundary Layer Meteorol.*, *78*, 87–119, 1996.

Mahrt, L., and M. Ek, The influence of atmospheric stability on potential evaporation, *J. Clim. Appl. Meteorol.*, *23*, 222–234, 1984.

Mahrt, L., and J. Sun, Multiple velocity scales in the bulk aerodynamic relationship for spatially averaged fluxes, *Mon. Weather Rev.*, *123*, 3032–3041, 1995.

McNaughton, K. G., and B. J. J. M. Van Den Hurk, A 'Lagrangian' revision of the resistors in the two-layer model for calculating the energy budget of a plant canopy, *Boundary Layer Meteorol.*, *74*, 261–288, 1995.

Monteith, J. L., and M. H. Unsworth, *Principles of Environmental Physics*, 291 pp., Edward Arnold, London, 1990.

Norman, J. M., and F. Becker, Terminology in thermal infrared remote sensing of natural surfaces, *Agric. For. Meteorol.*, *77*, 153–166, 1995.

Norman, J. M., W. P. Kustas, and K. S. Humes, A two-source approach for estimating soil vegetation energy fluxes from observations of directional radiometric surface temperature, *Agric. For. Meteorol.*, *77*, 263–293, 1995.

Otterman, J., J. Susskind, T. Brakke, D. Kimes, R. Pielke, and T. J. Lee, Inferring the thermal-infrared hemispheric emission from a sparsely-vegetated surface by directional measurements, *Boundary Layer Meteorol.*, *74*, 163–180, 1995.

Paulson, C. A., The mathematical representation of wind speed and temperature profiles in the unstable atmospheric surface layer, *J. Appl. Meteorol.*, *9*, 857–861, 1970.

Raupach, M. R., and J. J. Finnigan, Single-layer models of evaporation from plant canopies are incorrect but useful, whereas multilayer models are correct but useless, *Aust. J. Plant Phyiol.*, *15*, 705–716, 1988.

Sellers, P., and J. L. Dorman, Testing the simple biosphere model (SiB) using point micrometeorological and biophysical data, *J. Clim. Appl. Meteorol.*, *26*, 622–651, 1987.

Sellers, P., et al., The boreal ecosystem-atmosphere study (BOREAS): An overview and early results from the 1994 field year, *Bull. Am. Meteorol. Soc.*, *76*, 1549–1577, 1995.

Shuttleworth, W. J., and J. S. Wallace, Evaporation from sparse crops—An energy combination theory, *Q. J. R. Meteorol. Soc.*, *111*, 839–855, 1985.

Smith, E. A., et al., Area-averaged surface fluxes and their time-space variability over the FIFE experimental domain. *J. Geophys. Res.*, *97*, 18,599–18,622, 1992.

Stewart, J. B., Turbulent surface fluxes derived from radiometric surface temperature of sparse prairie grass, *J. Geophys. Res.*, *33*, 25,429–25,433, 1995

Stewart, J. B., W. P. Kustas, K. S. Humes, W. D. Nichols, M. S. Moran, and H. A. R. de Bruin, Sensible heat flux-radiometric surface temperature relationship for eight semiarid areas, *J. Appl. Meteorol.*, *33*, 1110–1117, 1994.

Sun, J., and L. Mahrt, Spatial distribution of surface fluxes estimated from remotely sensed variables, *J Appl. Meteorol.*, *33*, 1341–1353, 1994.

Sun, J., and L. Mahrt, Determination of surface fluxes from the surface radiative temperature, *J. Atmos. Soc.*, *52*, 1096–1106, 1995a.

Sun, J., and L. Mahrt, Relationship of the heat flux to microscale temperature variations· Application to BOREAS, *Boundary Layer Meteorol.*, *76*, 291–301, 1995b.

Tucker, C. J., Red and photographic infrared linear combinations for monitoring vegetation, *Remote Sens. Environ.*, *8*, 127–150, 1979.

Wallace, J. S., Calculating evaporation: Resistance to factors, *Agric For. Meteorol.*, *73*, 353–366, 1995.

Yoder, B. J., and R. H. Waring, The normalized difference vegetation index of small douglas-fir canopies with varying chlorophyll concentrations, *Remote Sens. Environ.*, *49*, 81–91, 1994.

R. L. Desjardins, Centre for Land and Biological Resource Research, Agriculture Canada, Ottawa, Ontario, K1A OC6, Canada.

N. O. Jensen, Department of Meteorology and Wind Energy, Risø National Laboratory, 4000 Roskilde, Denmark.

J. I. MacPherson, Flight Research Laboratory, National Research Council, Ottawa, Ontario, K1A OR6, Canada.

L. Mahrt, College of Oceanic and Atmospheric Sciences, Oregon State University, Corvallis, OR 97331. (e-mail: mahrt@ats.orst.edu)

J. Sun, Program in Atmospheric and Oceanic Sciences, University of Colorado, Boulder, CO 80309.

(Received March 19, 1996; revised December 19, 1996; accepted March 3, 1997.)